

Modeling and Fabrication of Heterogeneous Three-dimensional Objects based on Additive Manufacturing

Pu Huang, Dongping Deng, Yong Chen*
Epstein Department of Industrial and Systems Engineering
University of Southern California, Los Angeles, CA, USA

*Corresponding author: yongchen@usc.edu, (213) 740-7829

Abstract

Heterogeneous object modeling and fabrication has been studied in the past few decades. Recently the idea of digital materials has been demonstrated by using Additive Manufacturing (AM) processes. Our previous study illustrated that the mask-image-projection based Stereolithography (MIP-SL) process is promising in fabricating such heterogeneous objects. In the paper, we present an integrated framework for modeling and fabricating heterogeneous objects based on the MIP-SL process. Our approach can achieve desired grading transmission between different materials in the object by considering the fabrication constraints of the MIP-SL process. The MIP-SL process planning of a heterogeneous model and the hardware setup for its fabrication are also presented. Test cases including physical experiments are performed to demonstrate the possibility of using heterogeneous materials to achieve desired physical properties. Future work on the design and fabrication of objects with heterogeneous materials is also discussed.

Keywords: Heterogeneous Object, Material Design, Stereolithography, Functional Grading Material, Process Planning.

1. Introduction

An engineered heterogeneous object can be classified into three categories [1]. The first type is a multi-material object that is constructed by pieces of different materials with clear boundary between them [2]. The second is a functional-grading material object in which difference portions of material do not have clear boundary. Instead, they have a continuous transmission between them [3, 5]. The third one is an object with digital materials, in which different types of materials can be freely distributed in the object. The modeling and fabrication of such objects using digitally designed materials is the focus of this paper.

The main fabrication methods that can build the third type of heterogeneous objects are the recently developed Additive Manufacturing (AM) processes. For example, the AM processes such as multi-jet modeling, laser deposition manufacturing, and direct metal deposition have been demonstrated before in fabricating heterogeneous objects. In our previous work, the mask-image-projection based Stereolithography (MIP-SL) has also been demonstrated to be promising in fabricating heterogeneous objects with digital materials [4]. The research presented in this paper is mainly based on the MIP-SL process.

In the MIP-SL process, an input three-dimensional (3D) model is first sliced into layers of two-dimensional (2D) mask images. The generated mask images are then projected onto photosensitive resin that can be cured and accumulated to build a solid part. This process has been widely used in fabricating models with a single material. Our previous work extends the single material system into a multiple-material system. Heterogeneous objects in all the three categories can be fabricated by the multiple-material system [4]. A test example is shown in Figure 1. A heterogeneous object in computer-aided design (CAD) model is shown in Figure 1.a; the fabricated object using the MIP-SL process is shown in Figure 1.b, in which different colors indicate different materials. The shown object is a type one heterogeneous object as clear boundaries exist between the two types of materials.

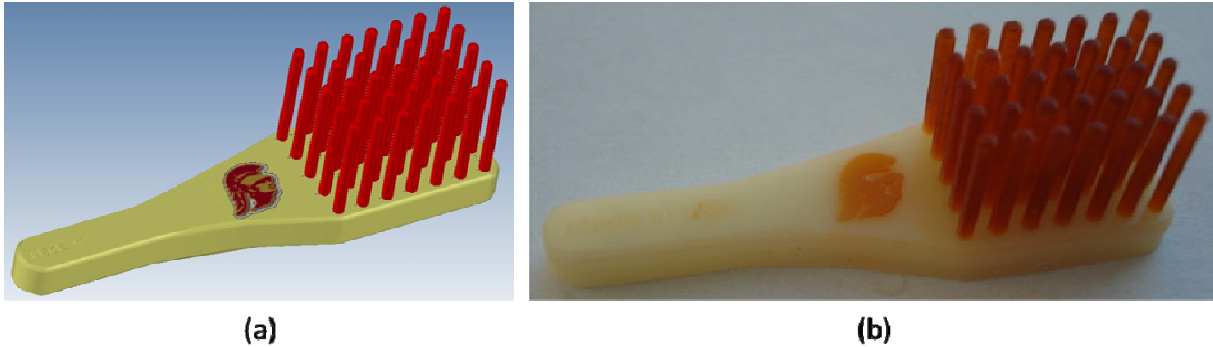


Figure 1: An example of a heterogeneous model fabricated by MIP-SL process [4]. (a) The CAD model of a multi-material design; (b) the fabricated object.

This paper presents an approach to model, analyze and fabricate heterogeneous objects based on the MIP-SL process. Our approach can handle all three types of heterogeneous objects. The problem definition of our approach is presented as follows.

Problem Definition: For a given 3D model M in triangular mesh, our approach allows user to define r control features $C_i, i \in [1, r]$ with each control feature associated with one type of material (note that multiple control features can exist for one type of material) and a material distribution function $F(u)$ for any given point \bar{x} in the space. The u is a r -dimensional vector with its element u_i as the closest distance between \bar{x} and C_i , i.e., $u_i = \min\|\bar{x} - x\|, x \in C_i$. Consequently, for any point $p \in M$, its corresponding material composition can be calculated by $m_p = F(u_p)$, where m_p is a k -dimensional vector that satisfies $\sum_{i=1}^k m_i = 1$ with k the number of material types. Accordingly the model M in heterogeneous materials defined by $F(u)$ is sliced with a set of planes. For each plane, k binary images $\{L_i\}, i \in [1, k]$ are generated with each L_i representing the mask images used in the MIP-SL process for material type i .

The work flow of the heterogeneous object modeling and fabrication framework is shown in Figure 2. After an STL mesh M is imported, its geometry is firstly converted into the LDNI representation [23]. The user can then design its heterogeneous distribution. The heterogeneous design is then analyzed by the Finite Element Analysis (FEA), and ask user to revise the design if necessary. Once the analysis result satisfies user requirements, process planning is performed to generate input mask images for the MIP-SL process. Finally, the heterogeneous part is fabricated. Without the loss of generality, we will use $k = 2$ (i.e. heterogeneous object with two types of materials) throughout the paper since our fabrication prototype

system is currently able to fabricate objects with two types of materials. However, the approach can easily be extended to $k > 2$ situations.

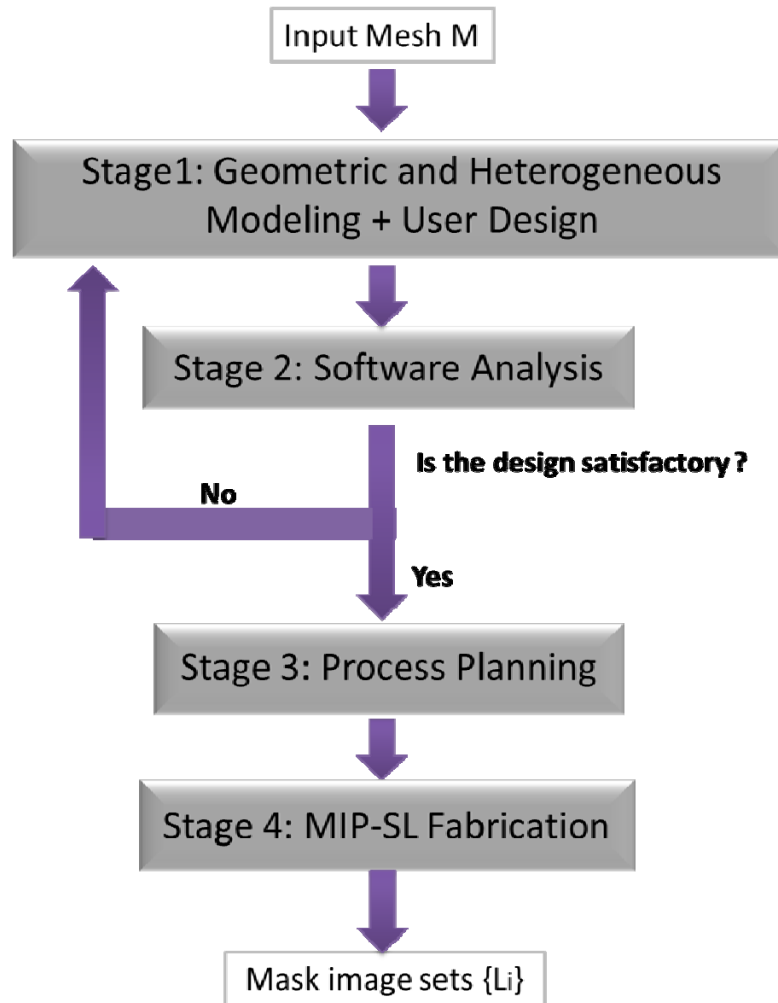


Figure 2: Work flow of our framework.

The technical contributions of the paper are:

1. An integrated framework is presented for modeling and fabricating heterogeneous objects based on the MIP-SL process;
2. A process planning method is developed to plan a set of 2D mask images for a defined heterogeneous model;
3. Experimental results are presented to demonstrate the capability of using heterogeneous materials in achieving physical properties.

The remainder of the paper is organized as follows. The related work is reviewed in Section 2. The geometric and heterogeneous modeling is presented in Section 3. The software analysis of the user designed heterogeneous model is discussed in Section 4. The process planning method is presented in Section 5. Our hardware setup for the heterogeneous MIP-SL process is described in Section 6. The experimental results and a case study are reported in Section 7. Finally the conclusions are drawn in Section 8.

2. Related Work

2.1 Heterogeneous Modeling

A lot of researches on the modeling of heterogeneous objects have been done before. Different models are used in the representation of heterogeneous material distribution such as voxel model, volume mesh model, implicit function model, explicit function model, control point model, etc. Tan [6] provides a comprehensive review of the heterogeneous modeling. According to [6], heterogeneous models could be classified into three categories: evaluated model, unevaluated model and composite model.

(1) Evaluated models present heterogeneous objects through intensive space subdivision. They can be further divided into two types. The first type is called voxel based model [7,8]. In voxel based model, the spatial material distribution is represented in a uniform 3D voxel grid with each voxel indicating the type of material in this unit grid. The second type is called volume mesh based model. It is similar to voxel model while it uses a collection of polyhedrons instead of spatial grids to represent 3D models [9,10]. Tetrahedron and hexahedrons are commonly used in volume mesh model.

(2) Unevaluated models represent heterogeneous distribution through rigorous mathematical expressions instead of spatial subdivision. Hence, unevaluated models are usually independent with resolution, i.e., unevaluated models can generate a model at any given precision. Unevaluated models generally fall into three categories: analytical functional representation, single feature based model, and multiple feature based model. Analytical functional representation utilizes explicit functions (e.g. Linear, quadratic, exponential) to represent the material composition for each position in a Cartesian coordinate [11]. It is obvious that such material distribution representation is independent of geometry descriptions since it is based on the coordinate system. Feature based models avoid the disadvantage of coordinate system dependence of analytic function representation mentioned above thus are more intuitive and straightforward in capturing users' intents. Siu and Tan [12] proposed a grading source representation for single feature based model. The grading source is defined as "origin of grading", and assigns the grading information such as material distribution function to a reference of the model. The "field of grading" is generated according to the source, and could be modified independent to geometry changes. Multiple control feature model extend from single control feature. It uses more than one control features as the material variation references to define material compositions [13,14].

(3) Composite model usually consists of both evaluated and unevaluated models. Evaluated model has advantage of big representing capacity. It can handle very complicated heterogeneous distribution. However, it usually suffers from memory and time efficiency problem. Unevaluated model are compact and exact since they use mathematical function to represent material composition distribution. In addition, they can provide efficient material composition evaluation for any given point by evaluating the function value. They are more intuitive to capture user's intent for design.

The unevaluated model was chosen in our approach since its representation capacity is enough to demonstrate heterogeneous object design and fabrication based on the MIP-SL process. An unevaluated model is more suitable for heterogeneous object design specified by users.

2.2 Heterogeneous Material Planning and Fabrication

A physical object can be fabricated by an additive manufacturing process based on a CAD model. So far the most popular AM process planning approach is to use a planar slicing plane to generate parallel scan lines. There are many issues related to the approach in the fabrication of heterogeneous objects. The first one is related to the slicing of the CAD models. Traditional assembly models that are directly used in fabricating heterogeneous objects have problems on the robustness and efficiency of the slicing algorithms [15]. Accordingly a heterogeneous cellular model is developed, which excludes the irrelevant boundary elements such that a heterogeneous model could be sliced as one single model rather than an assembly model. Hence the generating of parallel scanning lines is robust and efficient. A processing algorithm for freeform fabrication of heterogeneous structures is presented in [16]. A topological hierarchy-based approach to toolpath planning for multi-material layered manufacturing of heterogeneous objects is also presented in [17]. A topological hierarchy-sorting algorithm is used to group complex multi-material slice contours into families connected by a parent-and-child relationship. Subsequently, a sequential toolpath planning algorithm generates multi-toolpaths for sequential deposition of materials without redundant tool movements.

Various fabrication methods have been used in building heterogeneous objects, such as laser deposition [18], direct metal deposition [19], three dimensional printing (3DP) and micro droplets dispensing [20]. A digital-micromirror-device projection printing (DMD-PP) process [21] that is similar to our process is used in fabricating scaffolds for heterogeneous tissue engineering. The UV light curable polymer is also used in fabricating heterogeneous objects with controllable layer thickness [22].

3. Geometric and Heterogeneous Modeling

3.1 Geometric Modeling

Our prototype system import CAD models in STL format to define the model shape. After a STL model is imported, we will convert it into a solid representation called Layer Depth Normal Image (LDNI) [23]. The LDNI representation uses a set of well-organized points to implicitly represent the shape of the model. Since we will create two binary images on each slicing plane in the process planning, only the in/out classification for each point (i.e., pixel) on the binary image will be evaluated. An advantage provided by the LDNI representation is the efficient in/out classification such that the speed of our process planning can be significantly improved. The conversion from STL model into LDNI can be parallelized using hardware acceleration based on Graphical Processing Unit (GPU) [23].

3.2 Heterogeneous Modeling

As stated above, we will focus on the situation of $k = 2$ in this paper. Among the 2 types of material, the user should firstly choose one as background material which means the model will be initialized in homogeneous background material. Then, one or more control features for the other type of material can be specified by the user. For our approach, the control feature can be in any shape. In our prototype system, we temporarily allow user to define four types of control features: point, axis, plane and line segment. Figure 3 provides an illustration of the four types of control feature and a combination of three control features.

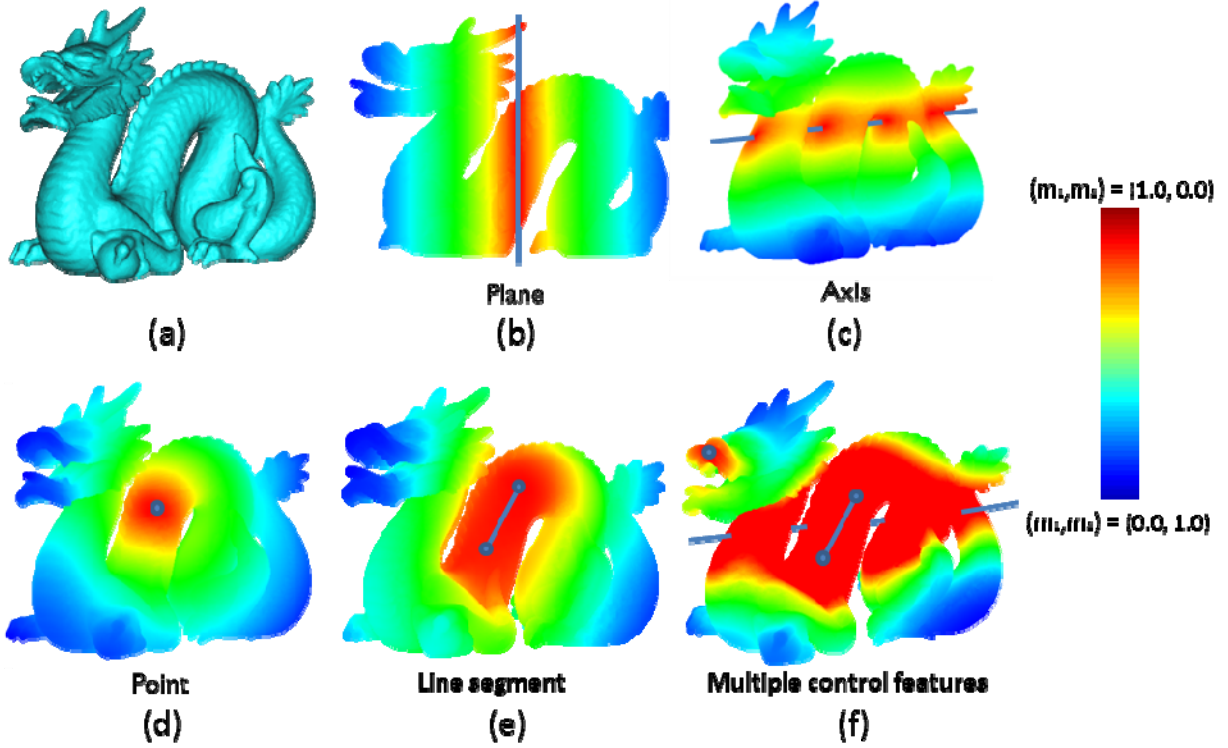


Figure 3: The illustration of different control features. (a) The original Dragon model; (b) the plane control feature; (c) the axis control feature; (d) the point control feature; (e) the line segment control feature; and (f) the combination of three control features: line segment, axis and point. Note that the control features are associated with material 1 (red) and the background material is set to be material 2 (blue).

Recall that for any given point $p \in M$, by defining function $F(u)$, we can have $m_p = F(u_p)$ where u_p and m_p are distance vector and material composition vector respectively associated with p . Suppose material 2 is selected as background material and there are r control features associated with material 1. The r -dimensional vector $u_p = (u_{p,1}, u_{p,2}, \dots, u_{p,r})$ in which $u_{p,i}, i \in [1, r]$ are the minimum distance from p to any material 1 control feature $C_i, i \in [1, r]$. The return vector $m_p = (m_{p,1}, m_{p,2})$ represents the material composition of material 1 and material 2 at point p with $u_{p,1}$ and $u_{p,2}$ indicating the percentage of their corresponding material. The function $F(u)$ basically calculate the percentage $m_{p,1}$ for material 1 at point p based on u_p . Then the percentage for background material, material 2 can be calculated simply by $1 - m_{p,1}$. Hence, function $F(u)$ can be represented by the following formula:

$$F(u_p) = (f(u_p), 1 - f(u_p)) = (m_{p,1}, m_{p,2}) \quad (1)$$

in which the function $f(u_p)$ is used to calculate $m_{p,1}$. It can be defined as follow:

$$f(u_p) = h(\sum_{i=1}^r g(u_{p,i})) \quad (2)$$

in which $g(u_{p,i})$ is elementary function associated with control feature C_i , it calculate the percentage of material 1 at point p under the influence of the control feature C_i . $h(x)$ is a regulating function which can be expressed as:

$$h(x) = \begin{cases} 1 & x > 1 \\ x & x \geq 0 \text{ and } x \leq 1 \\ 0 & x < 0 \end{cases} \quad (3)$$

It will guarantee the value of $m_{p,1}$ will be always in the range of $[0.0, 1.0]$. Hence $m_{p,1}$, the total percentage of material 1 at p is given by the regulated summation of the percentages under all the material 1 associated control features.

Our prototype system employs a novel way to intuitively define the influence function $g(u_{p,i})$ for control feature C_i . The influence range for C_i is constructed by two areas. The first area is called core area, it will have the material composition homogeneous as the material type that associated with C_i at any point in it. The second area is called the boundary area in which the percentage of C_i associated material decrease as the distance to C_i becomes larger. The user is free to control the radius of core area around C_i and the radius of boundary area around core area. In addition, the user has flexibility to define the transmission function for the boundary area, for example, linear or exponential functions. Figure 4 shows the effect of different radius of core area and boundary area.

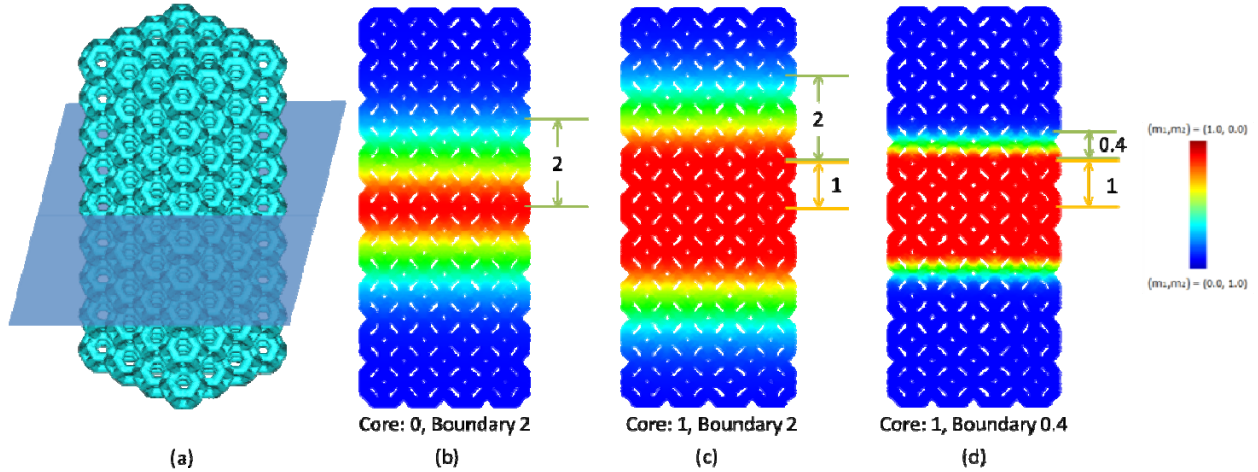


Figure 4: The effect of different radius of core area and boundary area. (a) The truss structure model and the control feature plane; (b) the core radius is 0 and the boundary radius is 2; (c) the core radius is 1 and the boundary radius is 2; (d) the core radius is 1 and the boundary radius is 0.4. Note that material 2 is the background material.

4. Heterogeneous Object Analysis

After a heterogeneous model is designed by users, it can be analyzed using simulation software systems such as COMSOL or ANSYS. The goal of this analysis is to verify whether the model can achieve desired physical properties. In this paper, we will demonstrate the potential of the MIP-SL fabricated heterogeneous models in achieving mechanical properties that cannot be achieved by a single material. Figure 5.(a) shows a simple test case, in which a bar with dimension $10cm \times 1cm \times 0.5cm$ is used. Suppose one end of the bar is fixed and a vertical force in $1N$ is applied at the other end. Planar control features are used in generating all the heterogeneous distributions but with their positions being different (refer to Figure 5.(b)-(g)). All the six models with heterogeneous material distributions are input into

COMSOL. A subdivision grid of $200 \times 20 \times 10$ with grid length $5 \times 10^{-4}m$ is applied on each bar. The Young's Module for the soft and hard material is set as 1.00×10^8 Pa and 2.68×10^9 Pa respectively. The value is selected according to the testing data of a rubber-like resin and IS500. Both resins are used in the MIP-SL process.

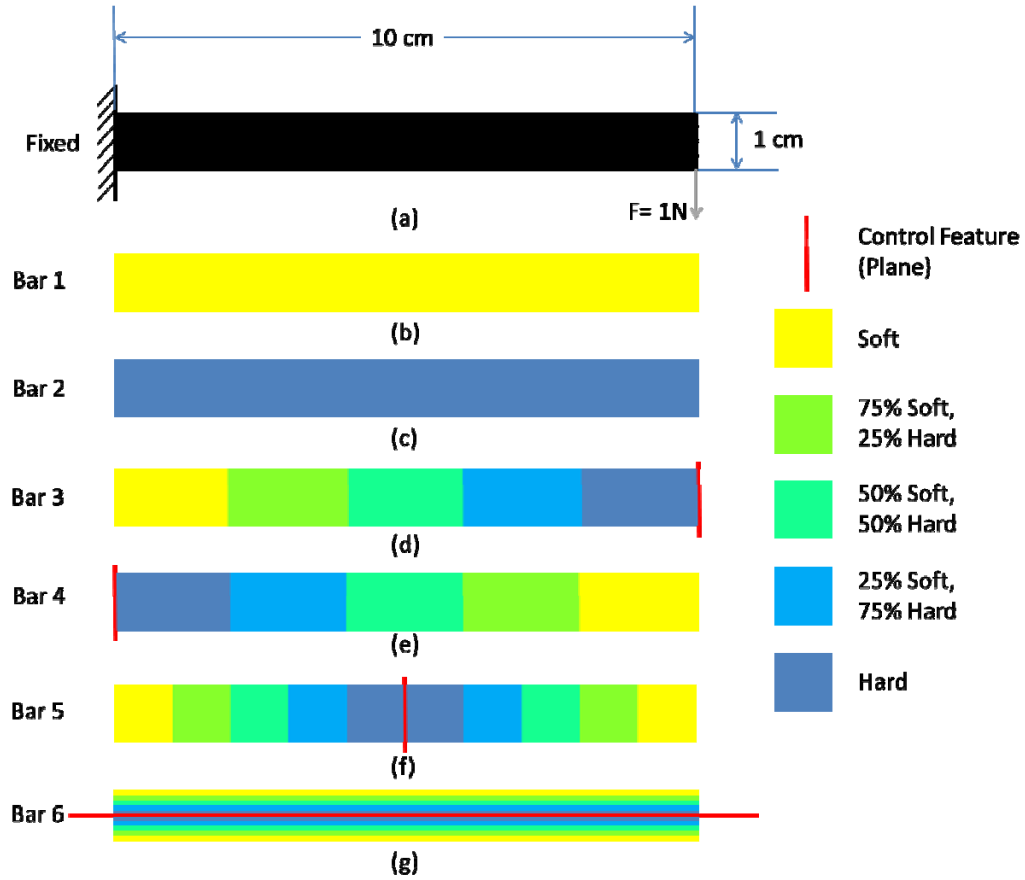


Figure 5: The geometry and heterogeneous distributions of the bars for FEA analysis. (a) The geometry and basic settings for FEA analysis for all bars; (b)-(g) heterogeneous distributions for bar 1-6 respectively.

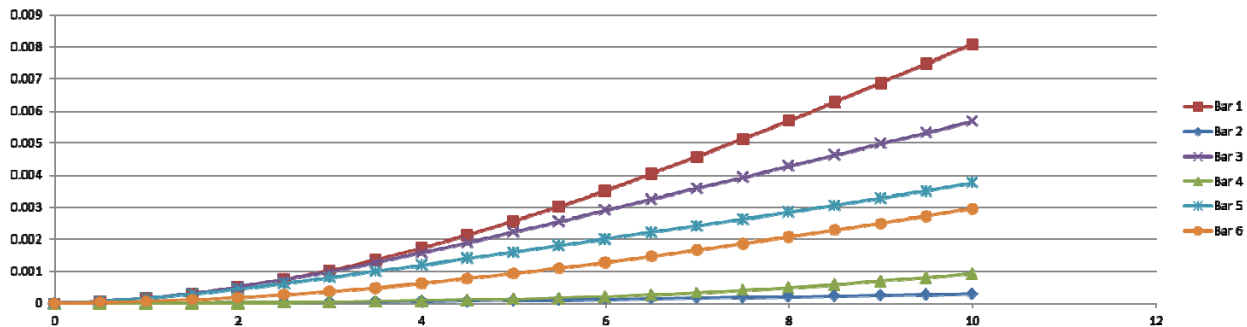


Figure 6: FEA analysis result in terms of bar deformation.

After running the simulation, the vertical displacements on 20 sampling points of each bar along horizontal direction are recorded. The simulation results are shown in Figure 6. As can be seen, the homogeneous soft and hard bar shows the largest and smallest vertical deformation. Bar 3 and Bar 4 are symmetric in terms of heterogeneous distribution. For bar 3, its curvature near the fixed end is larger than that of bar 4 due to its softness at this fixed end. However, at the other end of bar 3, its curvature is very small, makes its shape almost straight. While bar 4 shows little curvature at the fixed end, and larger curvature at the other end. It is obvious that the overall deformed shape of bar 3 and bar 4 is quite different since the larger deformation at the fixed end of bar 3 also contributes to that at the other end. This makes bar 3 has much larger vertical deformation at the free end. Bar 5 and bar 6 shows two other heterogeneous distributions which result in different deformed shape other than the previous 4 bars. It is easy to see that different heterogeneous distribution can result in different mechanical property. Hence, specific design of heterogeneous model can be used in achieving desired physical property in real applications. The design of material distribution for a given design requirement will be studied in our future work.

5. Process Planning for MIP-SL

In the multi-material based MIP-SL process, one mask image is used to define the shape of one specific material. Hence each layer will need two mask images in order to achieve the combination of two materials in the layer. In principle, the union of the two mask images for one layer should be the cross section image of the model on this layer (see Figure 7). Accordingly, for an input model, two sets of mask images L_1 and L_2 are prepared after slicing the model into a set of layers, with L_1 for material 1 and L_2 for material 2.

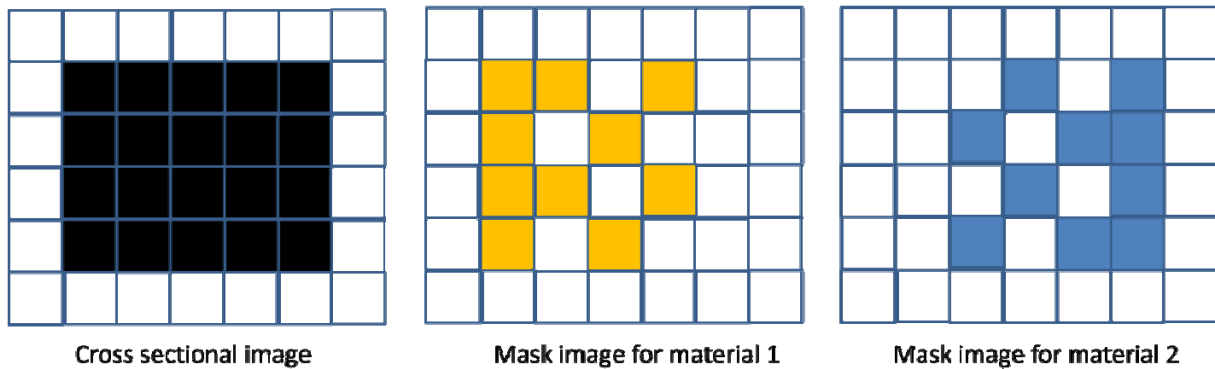


Figure 7: An example of mask images for material 1 and 2 for the same layer. Note that the union of the two mask images equals to the cross sectional region on this layer.

Due to the limitation of the MIP-SL process, the smallest feature that can be achieved in our MIP-SL system is 0.4 – 0.5mm. After calibration, each smallest feature is corresponding to 15 pixels on the mask image. Hence, the planned mask image can be decomposed into square pixel blocks with the block dimension of 15. The 15×15 pixel block is referred as unit block in this paper. Since we need to model the material composition of two types of materials, we should adapt the binary image to represent different material composition at certain position with these unit blocks. We further introduce a concept

of "giant block" for the material composition representation. One giant block consists of n^2 unit blocks in square pattern. In such a way, each giant block is able to represent $n^2 + 1$ different material composition layouts. Figure 8 gives an example of giant blocks that consist of 2^2 unit blocks for representing 5 different material compositions. Note that for the composition $(0.75, 0.25)$, $(0.5, 0.5)$ and $(0.25, 0.75)$, they have more than one configuration in binary image. When generating binary image, our approach will randomly choose one among the configurations listed in Figure 8 for certain composition. This randomization introduces the blending of different types of materials along the building direction in layered manufacturing. The $2d$ vector below each layout is the material composition m . Yellow and blue unit blocks indicate the physical unit of material 1 and 2 respectively. Note that n can easily be extended to a larger number. For example, one can use 3^2 unit blocks to form the giant block and get a representation that is capacity of 10 different composition layouts. In this paper, we use $n = 2$ for the demonstration in our examples.

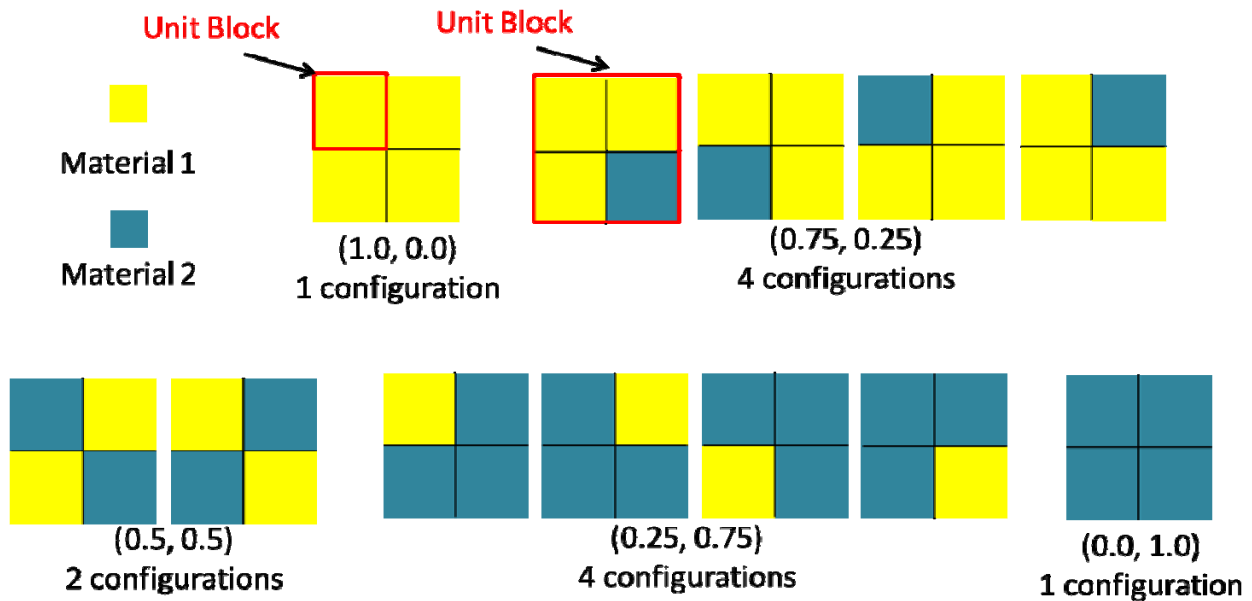


Figure 8: Five different material compositions represented by a giant block with dimension 2×2 in terms of unit blocks.

After defining the size of a giant block, slicing operation is applied on the model. For a specific slicing plane, two coincident binary images are created on the plane. The images are then decomposed into giant blocks and each giant block is further subdivided into several unit blocks. For each giant block, its in/out classification with respect to the LDNI solid definition is first evaluated by using its centroid as representative point. If a giant block is in the model, we will then further evaluate its material composition using this representative point. The calculated vector will be rounded to the closest composition vector available for the current giant block resolution. For example, for $n=2$, if the calculated material vector is $(0.74, 0.26)$, it will be approximated by the closest vector $(0.75, 0.25)$. Based on the material vector for specific giant block, the pre-defined configuration as shown in Figure 8 is applied to mask images related to materials 1 and 2. Consequently, two binary images will be generated for one layer. Due to the distribution of light intensity, the cured region is slightly larger than the white region on

binary image. Hence we apply an erosion operation in order to shrink the white region on the mask image as compensation. Figure 9 shows the erosion effect on the mask image. By applying the above stated procedure layer by layer, two sets of mask images can be calculated for the fabrication process.



Figure 9: Erosion effect on a mask image. (a) The mask image before erosion; (b) the mask image after erosion.

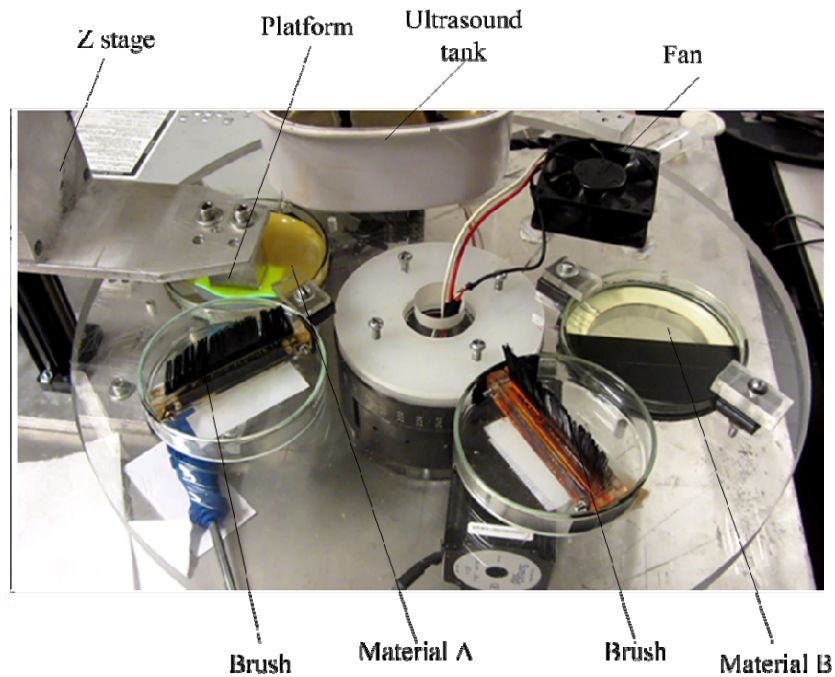


Figure 10: The rotary fabrication system.

6. Hardware Setup and Fabrication Process

Figure 10 shows a two-material MIP-SL prototype system based on a rotary table design. Main components of the system include a control board, an optical system, a Z-stage, a rotary stage and power supply. A platform for parts to be built on is mounted on the Z-stage. Two resin tanks are mounted on the rotary stage. A cleaning system including two brushes, a ultrasound cleaner and a fan are also mounted on the rotary stage. The ultrasound cleaner is used to remove resin residue on the part surface by vibrating alcohol solution to create micro-bubbles. The fan dries the alcohol left on the part after taking it out from the ultrasound cleaner. This process takes over 3 minutes to finish one layer. Alternate cleaning approaches were tested in order to speed up the process. Instead of ultrasound cleaning, a cotton pad

cleaning procedure is used in removing the residual resin. The fabrication process can be faster since the cotton pad cleaning procedure is simpler. However, it was found that there is still a rather thin layer of resin remained on the part after the cleaning process.

As the overall effect is good enough for our testing purpose, the new cleaning process is adopted. Two cotton pads are mounted on the rotary stage to clean the two types of resins. To avoid resin contamination, a post-curing step is used by exposing the part to a mask image to cure all residual resin after the cleaning process. Hence, the fabrication process follows the following steps. For each layer with two material compositions, first, the material *A* portion is cured; the rotary stage is then rotated to get the platform to the cotton pad *A*; the built part is rubbed against the pad to transfer resin residue to it; after that, the part is post-cured to thoroughly remove remaining liquid resin. The platform is then moved to the material *B* tank and the material *B* portion is fabricated. Similar procedure is repeated until the layer is built. It takes around 2 minutes to build a layer. When building of the next layer, the fabricating order will be reversed, i.e. the material *B* portion will be built before the material *A* portion. In such a way, an object can be fabricated after all the layers are built.

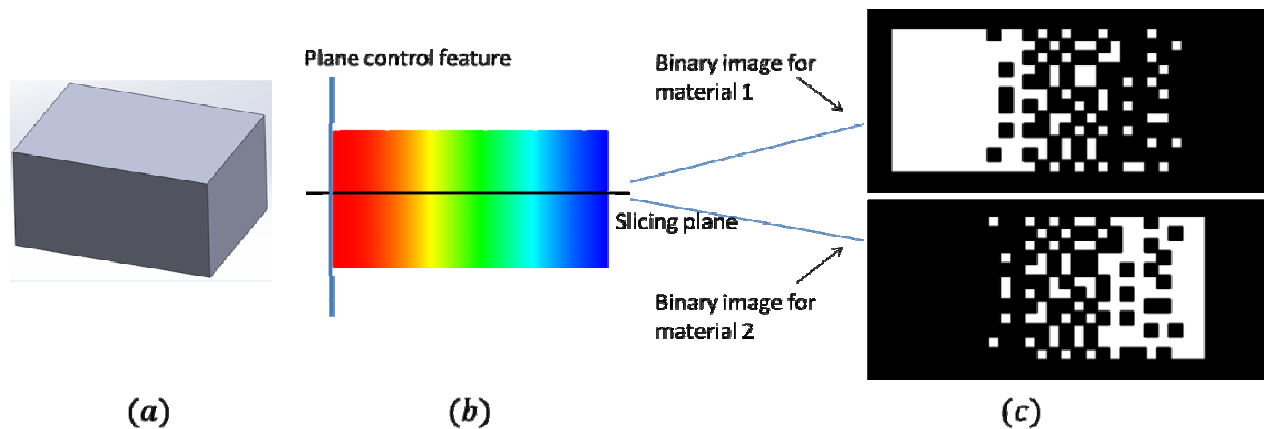


Figure 11: An example of a heterogeneous rectangular box. (a) The CAD model of the input rectangular box; (b) the heterogeneous distribution of the user design with a planar control feature; (c) mask images for material 1 and 2 for a specific layer.

7. Results and Discussion

In this section, we show some results of our prototype system. Figure 11 shows an example of a rectangular box. The control feature is a plane at the middle of the model. For a specific slicing image, it shows the mask images for both material 1 and material 2. Note that the union of these two mask images will form the entire cross sectional region on this slicing layer.

Three models of the case study discussed in Section 4 were fabricated using our prototype system to verify their mechanical properties. Two of them are homogeneous parts (transparent rubber and SI500) while the third one is a heterogeneous object with planer control feature and linear transmission pattern from SI500 to transparent rubber. The dimension of the three parts is $20\text{mm} \times 9\text{mm} \times 1.5\text{mm}$. We fix one end of the part and apply a vertical force in about 1N at the other end. Figure 12 shows the testing result. As can be seen from the figures, the deformed shapes of the three parts are quite different, and are consistent to our analysis results.

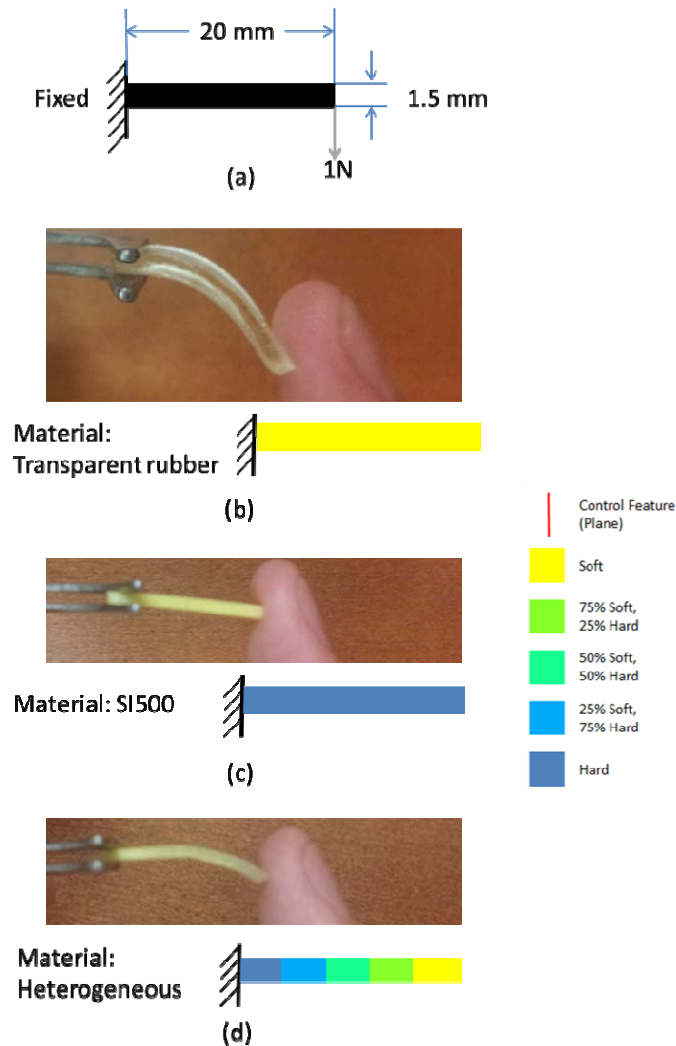
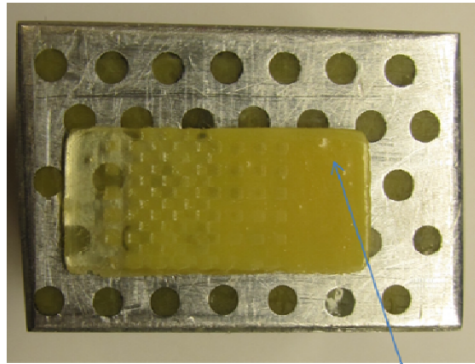


Figure 12: A case study of fabricated parts. (a) The dimension of testing part and testing setup; (b) the deformation of the transparent rubber bar; (c) the deformation of the SI500 bar; (d) the deformation of a heterogeneous bar with the 100%-SI500 end fixed.

For our fabricated parts, we use the 2^2 giant block which can represent 5 different material compositions. In fact, giant block containing more unit blocks can be used to obtain more representable material compositions and thus, make the material transmission smoother. Because of the limitation of fabrication process, the minimal unit we can fabricate is 0.5mm . This makes our unit block of $0.5 \times 0.5\text{mm}$ to be relatively large for heterogeneous object fabrication. We are investigating strategies to reduce the minimal fabricated unit size in order to get finer material composition result. In addition, the cleaning effect of the cotton is not very good because the cleaned resin will accumulate on the cotton pad and make it wet. Consequently when the process goes on, the cleaning effect becomes worse. In addition, some portion of the surface can be uneven during the fabrication process (refer to Figure 13). This may be due to the process of changing material tanks during the fabrication of a same layer. Cleaning approaches are under investigation to improve the cleaning effect and to reduce the fabrication time.



Uneven surface

Figure 13: The uneven surface on fabricated part.

8. Conclusion

In this paper, we presented a framework for the design and fabrication of heterogeneous objects based on the MIP-SL process. Our approach can achieve desired grading transmission between different materials. The fabrication constraints related to the MIP-SL process were discussed. They are incorporated in the developed framework. We also demonstrated the possibility of using heterogeneous material distribution in the fabricated object to achieve desired mechanical properties. The MIP-SL process planning of heterogeneous models and the hardware setup for heterogeneous model fabrication were discussed. Several test cases were presented to illustrate the benefits of digital material design.

Some future work that are under investigation includes (1) extending the current single control feature framework to multiple control features; (2) developing fully or partially automatic design approach to design heterogeneous material distribution according to the user specified physical properties; and (3) investigating strategies to reduce the minimal feature size in the fabrication process and to improve the fabrication speed.

Acknowledgement

The research conducted in this paper is partially supported by National Science Foundation CMMI-1151191 and CMMI-0927397.

Reference

- [1] Zhou H., Liu Z., and Lu B., Heterogeneous object modeling based on multi-color distance field, *Materials and Design*, 30(4), 939-946, 2009.
- [2] Kumar V., and Dutta D., An approach to modeling multi-material objects, *Proceedings of the fourth ACM symposium on Solid modeling and applications*, 336-345, 1997.
- [3] Zhou M. Y., Xi J. T., and Yan J. Q., Modeling and processing of functionally graded materials for rapid prototyping, *Journal of Materials Processing Technology*, 146(3), 396-402, 2004.
- [4] Zhou C., Chen Y., Yang Z., and Khoshnevis B., Digital Material Fabrication Using Mask-Image-Projection-based Stereolithography, *Rapid Prototyping Journal*, Vol. 19, No. 3, 2013.

- [5] Xu A. and Shaw L., Equal distance offset approach to representing and process planning for solid freeform fabrication of functionally graded materials, *Computer-aided Design*, 37(12), 1308-18, 2005.
- [6] Kou X. Y., Tan S. T., Heterogeneous object modeling: A review, *Computer-Aided Design*, 39(4), 284-301, 2007.
- [7] Chen M., and Tucker J. V., Constructive Volume Geometry, *Computer Graphics Forum*, 19, 281-293, 2000.
- [8] Vijay C., Manohar S., and Prakash C. E., Voxel-based modeling for layered manufacturing, *Computer Graphics and Applications*, IEEE, 15(6), 42-47, 1995.
- [9] Jackson, T. R., Analysis of Functionally Graded Material Object Representation Methods, Thesis (Ph.D.)--Massachusetts Institute of Technology, Dept. of Ocean Engineering, 2000.
- [10] Shin, K. H., Representation and process planning for layered manufacturing of heterogeneous objects, University of Michigan, 2002.
- [11] Zhu F., Visualized CAD modeling and layered manufacturing modeling for components made of a multiphase perfect material, These (Master of Philosophy)--The University of Hong Kong, Dept. of Mechanical Engineering, 2004.
- [12] Siu Y. K. and Tan S. T., Source-based heterogeneous solid modeling. *Computer-Aided Design*. 34(1), 41-55, 2002.
- [13] Biswas A., Shapiro V., and Tsukanov I., Heterogeneous material modeling with distance fields, *Computer-Aided Geometric Design*, 21(3), 215-242, 2004.
- [14] Samanta K. and Koc B., Feature-based design and material blending for free-form heterogeneous object modeling, *Computer-Aided Design*, 37(3), 287-305, 2005.
- [15] Kou X. Y., Tan S. T., Robust and efficient algorithms for rapid prototyping of heterogeneous objects, *Rapid Prototyping Journal*, 15(1), 5-18, 2009.
- [16] Sun W., Jiang T., and Lin F., A processing algorithm for freeform fabrication of heterogeneous structures, *Rapid Prototyping Journal*, 10(5), 316-326, 2004.
- [17] Choi S. H. and Cheung H. H., A topological hierarchy-based approach to toolpath planning for multi-material layered manufacturing, *Computer-Aided Design*, 38(2), 143-156, 2006.
- [18] Hu Y., Blouin V. Y., Fadel G. M., Incorporating manufacturability constraints into the design process of heterogeneous objects, *Intelligent Systems in Design and Manufacturing*, Proceedings of the SPIE, 5605, 214-225, 2004.
- [19] Hejimiadi U. and McAlea K., Selective Laser Sintering of Metal Molds: The RapidTool Process, *Solid Freeform Fabrication Symposium*, Texas, August 12th-14th, 1996.
- [20] Zhu Y. F, Peng C., Yang J. Q., Wang C. M., An Integrated Design and Fabrication Approach for Heterogeneous Objects, *Advanced Materials Research*, 383, 5810-5817, 2011
- [21] Han L. H., Suri S., Schmidt C. and Chen S., Fabrication of three-dimensional scaffolds for heterogeneous tissue engineering, *Biomedical Microdevices*, 12(4), 721-725, 2010.
- [22] Lee S. A., Chung S. E., Park W. and et al., Three-dimensional fabrication of heterogeneous microstructures using soft membrane deformation and optofluidic maskless lithography, *Lab Chip*, 9(12), 1670-1675, 2009.

- [23] Chen Y., Wang C. C. L., Layer Depth-Normal Images for Complex Geometries - Part I: Accurate Modeling and Adaptive Sampling, Proceedings of ASME Design Engineering Technical Conferences, DETC2008-49432, Brooklyn, New York, 2008.